

## ARTICLE



# Role of angiogenesis in beta-cell epithelial–mesenchymal transition in chronic pancreatitis-induced diabetes

Jieqi Qian<sup>1,2</sup>, Dongdong Tao<sup>3</sup>, Xiaou Shan<sup>1</sup>✉, Xiangwei Xiao<sup>2</sup>✉ and Congde Chen<sup>1,2,3</sup>✉

© The Author(s), under exclusive licence to United States and Canadian Academy of Pathology 2021

Clinical evidence suggests that patients with chronic pancreatitis (CP) are prone to development of diabetes (chronic pancreatitis-related diabetes; CPRD), whereas the underlying mechanisms are not fully determined. Recently, we showed that the gradual loss of functional beta-cells in a mouse model for CPRD, partial pancreatic duct ligation (PDL), results from a transforming growth factor  $\beta$ 1 (TGF $\beta$ 1)-triggered beta-cell epithelial–mesenchymal transition (EMT), rather than from apoptotic beta-cell death. Here, the role of angiogenesis in CPRD-associated beta-cell EMT was addressed. We detected enhanced angiogenesis in the inflamed pancreas from CP patients by bioinformatic analysis and from PDL-mice. Inhibition of angiogenesis by specific antisera for vascular endothelial growth factor receptor 2 (VEGFR2), DC101, did not alter the loss of beta-cells and the fibrotic process in PDL-pancreas. However, DC101-mediated inhibition of angiogenesis abolished pancreatitis-induced beta-cell EMT and rendered it to apoptotic beta-cell death. Thus, our data suggest that angiogenesis promotes beta-cell survival in the inflamed pancreas, while suppression of angiogenesis turns beta-cell EMT into apoptotic beta-cell death. This finding could be informative during development of intervention therapies for CPRD.

*Laboratory Investigation* (2022) 102:290–297; <https://doi.org/10.1038/s41374-021-00684-5>

## INTRODUCTION

The endocrine islets and the exocrine pancreas comprise the pancreas organ<sup>1</sup>. This specific organization of pancreas could be the basis of the findings that some exocrine pancreatic diseases affect the functionality of islets. For example, patients with chronic pancreatitis (CP) have a greater chance to form pancreatic fibrosis and have a much higher risk of developing pancreatic ductal adenocarcinoma (PDAC)<sup>2</sup>. On the other hand, the CP-patients are also prone to glucose intolerance, peripheral insulin resist, and even diabetes, which is called chronic-pancreatitis-related diabetes (CPRD)<sup>3</sup>.

The mechanisms underlying CPRD are, however, not fully determined. Recently, we have used partial pancreatic duct ligation (PDL)<sup>4,5</sup> as a model to study CPRD in mice. For PDL, the pancreatic duct is ligated at the middle, preventing the ductal fluid from draining into common bile duct and thus causing the auto-digestion of the exocrine acinar cells by the digestive enzymes in the ductal fluid<sup>6</sup>. Severe inflammation is then induced specifically in the ligated tail part of the pancreas (PDL-tail) with the non-ligated head part of the pancreas (PDL-head) intact<sup>7,8</sup>. We have detected a gradual loss of functional beta-cells in PDL-tail after PDL, likely resulting from a transforming growth factor  $\beta$ 1 (TGF $\beta$ 1)-triggered beta-cell epithelial–mesenchymal transition (EMT), rather than from apoptotic beta-cell death<sup>9</sup>.

Studies of molecular signaling pathways in cancer have highlighted the interaction among inflammation, EMT and angiogenesis<sup>10,11</sup>. Angiogenesis is regulated by different pro-angiogenic factors,

among which vascular endothelial growth factor (VEGF) family members play a pivotal role<sup>12</sup>. We have previously reported the importance of VEGF-regulated angiogenesis in beta-cell homeostasis<sup>13,14</sup> and postnatal beta-cell growth<sup>15</sup>. Nevertheless, it is not known whether angiogenesis plays a role in the inflammation-induced beta-cell EMT<sup>9</sup>. This question was addressed in the current study.

Here, we detected enhanced angiogenesis in the inflamed pancreas from CP patients by bioinformatic analysis and from PDL-mice. In a loss-of-function approach, angiogenesis was specifically inhibited by antisera against vascular endothelial growth factor receptor 2 (VEGFR2), commercially named DC101, which have been widely used to suppress angiogenesis in numerous studies<sup>16–18</sup>. DC101 did not alter the loss of beta-cells and the fibrotic process in PDL-pancreas. However, DC101-mediated inhibition of angiogenesis abolished pancreatitis-induced beta-cell EMT and rendered it to apoptotic beta-cell death.

## MATERIALS AND METHODS

### Mouse manipulation

All mouse experiments were approved by the Animal Research and Care Committee at the Children's Hospital of Pittsburgh and the University of Pittsburgh IACUC. *INS1<sup>cre</sup>* knock-in<sup>19</sup>, *Rosa26CAGTomato* (TOM)<sup>13</sup>, *MIP-GFP<sup>20</sup>*, TGF $\beta$  receptor II (TBR2) *fx/fx<sup>7</sup>*, and C57BL/6 mice have been described before<sup>9,15,21,22</sup>. Male and female mice were all used in experiments at 10 weeks of age and were well distributed in the group.

<sup>1</sup>Department of Pediatric Endocrinology, the Second Affiliated Hospital and Yuying Children's Hospital of Wenzhou Medical University, Wenzhou 325000, China. <sup>2</sup>Department of Surgery, Children's Hospital of Pittsburgh, University of Pittsburgh School of Medicine, Pittsburgh, PA 15224, USA. <sup>3</sup>Department of Pediatric Surgery, the Second Affiliated Hospital and Yuying Children's Hospital of Wenzhou Medical University, Wenzhou 325000, China. ✉email: 2296037178@qq.com; xiangwei.xiao@chp.edu; chencd@wmu.edu.cn

Received: 23 June 2021 Revised: 30 September 2021 Accepted: 1 October 2021

Published online: 11 November 2021

PDL was performed and validated as described<sup>7,8</sup>. Briefly, the middle of the main pancreatic duct was surgically ligated in mice to allow the non-ligated pancreatic head to weigh about 45% of the total pancreas. DC101 and control rat IgG were purchased from Antibodies.com (A250834). For each i.p. injection, 750 ng/25 mg body weight was used.

**Pancreatic digestion, islet isolation and flow cytometry**

Pancreas was digested with collagenase P (Sigma-Aldrich, Carpinteria, CA, USA) followed by gradient centrifugation using histopaque 1110 prepared by mixing histopaque 1119 and 1077 (Sigma-Aldrich). Islets were picked by hand from the supernatant. The beta-cells were purified from dissociated islet cells from INS1<sup>Cre</sup>, TOM; MIP-GFP mice, based on direct fluorescence for GFP and TOM, as described<sup>7,8,13,14</sup>. Cell sorting was performed with a BD FACSAria II flow cytometer (Becton-Dickinson Biosciences, San Jose, CA, USA). The flow cytometry data were analyzed by Flowjo (version 11.0, Flowjo LLC, Ashland, OR, USA).

**Isolation of RNA and RT-qPCR**

RNA extraction was performed using a RNeasy kit (Qiagen), and RT-qPCR were performed with a SYBR Green assay, as described previously<sup>7,8,13,14</sup>.

Primers were all purchased from Qiagen (Valencia, CA, USA), including Cyclophilin A (QT00247709), E-cadherin (QT00121163), Snail (QT00240940), Slug (QT00098273), ZEB1 (QT00105385) and ZEB2 (QT00148995). RT-qPCR values were obtained by sequential normalization against Cyclophilin A and the experimental control conditions (normalized as 1).

**Histology, TUNEL assay, Western blot and immunohistochemistry**

Pancreas was fixed in 4% formaldehyde (PFA) for 6 h, and cryo-protected in 30% sucrose overnight before embedding, as described before<sup>7</sup>. Masson-trichrome staining was performed using a Trichrome Stain (Masson) Kit (Sigma-Aldrich). TUNEL assay was done using a specific detection kit (Roche Applied Science, Nutley, NJ, USA)<sup>9</sup>. The percentage of apoptotic beta-cells was calculated by dividing total insulin+ beta-cells with TUNEL + insulin+ beta-cells. GFP and TOM were detected by direct fluorescence. For Western blot, total protein was extracted from isolated islets with RIPA buffer (Sigma-Aldrich). The primary antibodies for Western Blot are rabbit polyclonal anti-GAPDH (#5174, Cell signaling Technology, Inc., Danvers, MA, USA) and rabbit polyclonal anti-Cleaved Caspase-9 (#9507, Cell signaling Technology, Inc.). The secondary antibody is HRP-conjugated

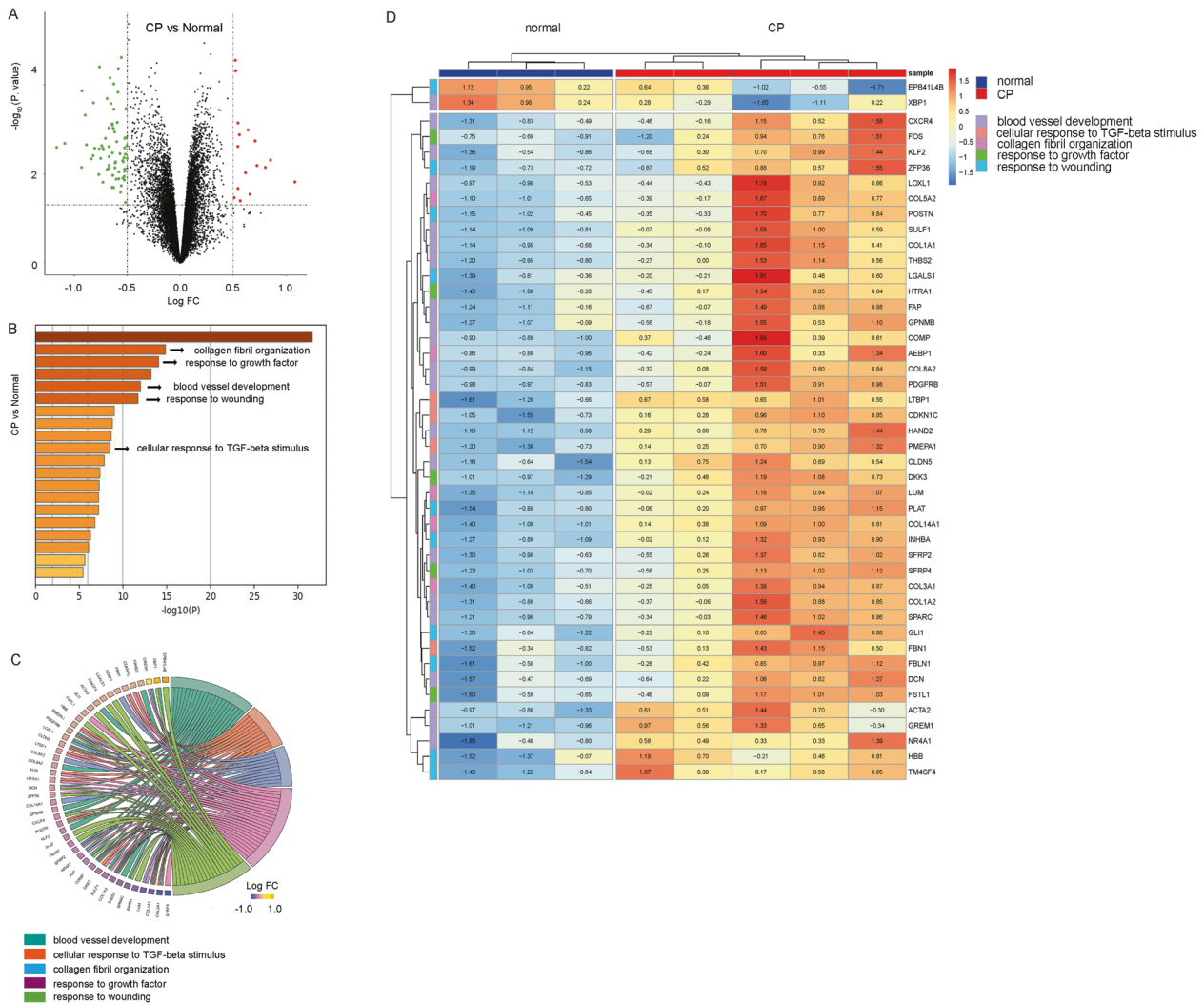


**Fig. 1 PDL is a model for both acute and chronic pancreatitis in humans.** Data from public database GSE77858 were obtained and analyzed with online tool GEO2R to screen DEGs. Pancreas from CP patients (n = 5) and normal human (n = 3) was compared. **A** An overview of gene expression was displayed in volcano plots, with red colored dots representing significantly upregulated genes and green colored dots representing significantly downregulated genes (P.value < 0.05 and |log2FC| > 0.5). **B** The top 20 enriched pathways analyzed by KEGG and GO databases. **C, D** A chord chart (**C**) and a heatmap (**D**) with clustering showing the relationship among differentially expressed genes and pathways including blood vessel development, collagen fibril organization, response to growth factor, response to wounding and cellular response to transforming growth factor beta stimulus.

anti-rabbit (Jackson ImmunoResearch Labs, West Grove, PA, USA). For immunohistochemistry, no antigen retrieval was required. The primary antibodies were guinea pig polyclonal anti-insulin (Dako, Carpinteria, CA, USA) and rat polyclonal anti-CD31 (Becton-Dickinson Biosciences). Rat and guinea pig -specific secondary antibodies were applied for indirect fluorescent staining (Jackson ImmunoResearch Labs). Nuclear staining was performed with 4',6-diamidino-2-phenylindole (DAPI, Becton-Dickinson Biosciences). Beta-cell mass was calculated by the pancreatic weight multiplied by the ratio of the insulin+ cell area versus the total pancreatic area. At least 4 slides with a distance of 100  $\mu\text{m}$  from each other were analyzed to avoid repeated calculation on the same cells/islets. The vessel density quantification was done similarly, albeit based on CD31 staining. These quantifications have been described in detail previously<sup>7,13</sup>.

### Bioinformatics

Data from public database were obtained from the Gene Expression Omnibus (GEO, <http://www.ncbi.nlm.nih.gov/geo/>)<sup>23</sup>. The data surf applied "carcinoma, pancreatic ductal" OR "carcinoma, pancreatic ductal" OR "carcinoma, pancreatic ductal" OR "Pancreatic Ductal Carcinoma\*" OR "PDAC" OR "Chronic Pancreatitis" OR "CP" AND "Homo sapiens". A total of 441 series for human CP or PDAC were retrieved from the database. After a careful comparison for relatedness, two gene expression profiles (GSE77858 and GSE61166) were selected<sup>24</sup>. Next, the GEO2R online analysis tool was used to detect the differentially expressed genes (DEGs), after which the *P* value, adjusted *P*-value and logFC were calculated. In the series of GSE77858, genes that met the cutoff criteria (*P* value < 0.05 and |logFC|  $\geq$  0.4) were selected as DEGs. In the series of GSE61166, genes that met the cutoff criteria (adjusted *P* value < 0.05 and |logFC|  $\geq$  2.0) were selected as DEGs. Pathway enrichment analyses of DEGs were performed at Metascape (<http://metascape.org>) and KEGG<sup>25</sup>. Terms with a *P* value < 0.01, a minimum count of 3, and an enrichment factor > 1.5 were collected and grouped into clusters based on their membership similarities (Kappa scores > 0.3). The most statistically significant term within a cluster was chosen to represent the cluster. If more than 20 terms for GO or pathway annotations were identified, only the top 20 terms were shown. We chose the R packages of "ggplot2", "pheatmap", "clusterProfiler" and "GOplot" to visualize DEGs and the enrichment pathways.

### Data analysis

Data analysis was performed in GraphPad Prism 7 (GraphPad Software, San Diego, CA, USA). All values were depicted as mean  $\pm$  standard deviation (SD) of the mean. Each experiment groups had 5–6 mice. All data were statistically analyzed using one-way ANOVA with a Bonferroni correction, followed by Fisher's exact test. Significance was considered when *p* < 0.05. Non-significance (NS) was shown when *p* < 0.05 was not met.

## RESULTS

### Evidence of enhanced angiogenesis in CP from public database

Previous reports showing the importance of angiogenesis to inflammation and EMT promoted us to investigate angiogenesis in long-term PDL, the model for CP. First, we obtained data from public database and used online tool GEO2R to screen DEGs when compared samples from pancreatitis patients (*n* = 5) and samples from normal human (*n* = 3). A total 84 DEGs were identified from GSE77858 datasets (Fig. 1A). Among these DEGs, there were 68 downregulated genes and 16 upregulated genes. Pathway enrichment analysis and protein-protein interaction network were assessed using Metascape online tool, showing that the enriched pathways were blood vessel development, collagen fibril organization, response to growth factor, response to wounding and cellular response to transforming growth factor beta (TGFB) stimulus (Fig. 1B–D). These data suggest enhanced angiogenesis in the pancreas from CP patients.

### Evidence of enhanced angiogenesis in tail-pancreas from PDL-mice

Next, we examined whether angiogenesis is also enhanced in the mouse model for CP, long-term PDL. PDL-tail mice were examined for CD31, a marker for endothelial cells, at 1w, 8w and 24w after surgery, compared to the sham-operated control. We found that, compared to sham, vessel density increased in both the islet region (representing endocrine pancreatic part) and the exocrine region (representing exocrine pancreatic part) at the examined time points (Fig. 2A,B). Moreover, the vessel area did not alter with time (Fig. 2A,B). These data suggest that PDL-induced pancreatic inflammation results in enhanced angiogenesis to maintain a sustained vessel density.

### Experimental suppression of angiogenesis does not alter post-PDL fibrosis

To check the importance of angiogenesis in long-term PDL model, we inhibited angiogenesis with specific antisera for VEGFR2, commercially named DC101, which have been widely used to suppress angiogenesis in numerous studies<sup>16–18</sup>. Moreover, *INS1<sup>cre</sup>*; Tom; MIP-GFP mice were used. In these mice, all beta-cells that are actively expressing insulin are green-fluorescent due to specific beta-cell-expression of GFP, while all beta-cells that have ever expressed insulin are red fluorescent due to occurrence

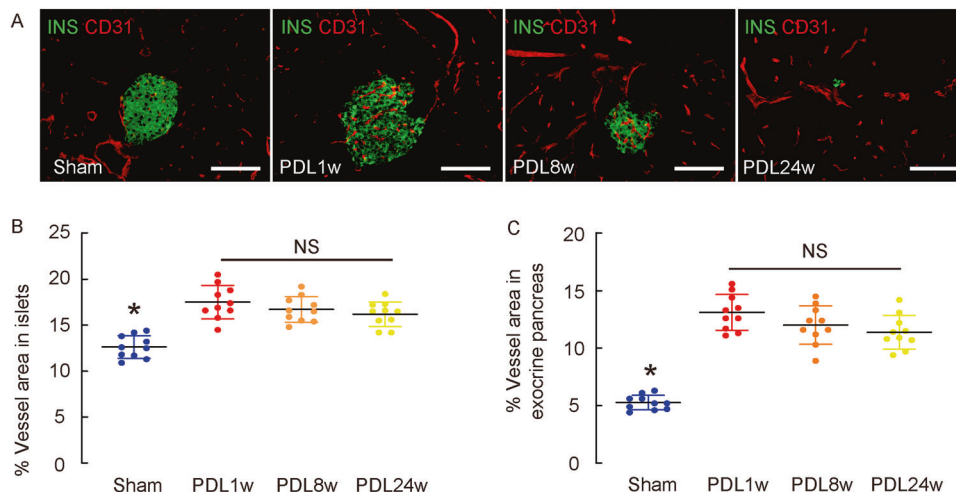


**Fig. 2 Evidence of enhanced angiogenesis in tail-pancreas from PDL-mice.** Tail pancreas from PDL mice was examined for CD31, a marker for endothelial cells, at 1w, 8w and 24w after surgery, compared to sham-operated control. **A–C** Vessel density was determined based on immunostaining for CD31 and insulin, shown by representative immunofluorescent images (**A**), and by quantification in islet area (**B**) and in exocrine pancreas (**C**). Each condition contained 10 age-matched mice, five male and five female. \**p* < 0.05. NS non-significant. Scale bars are 100  $\mu\text{m}$ .

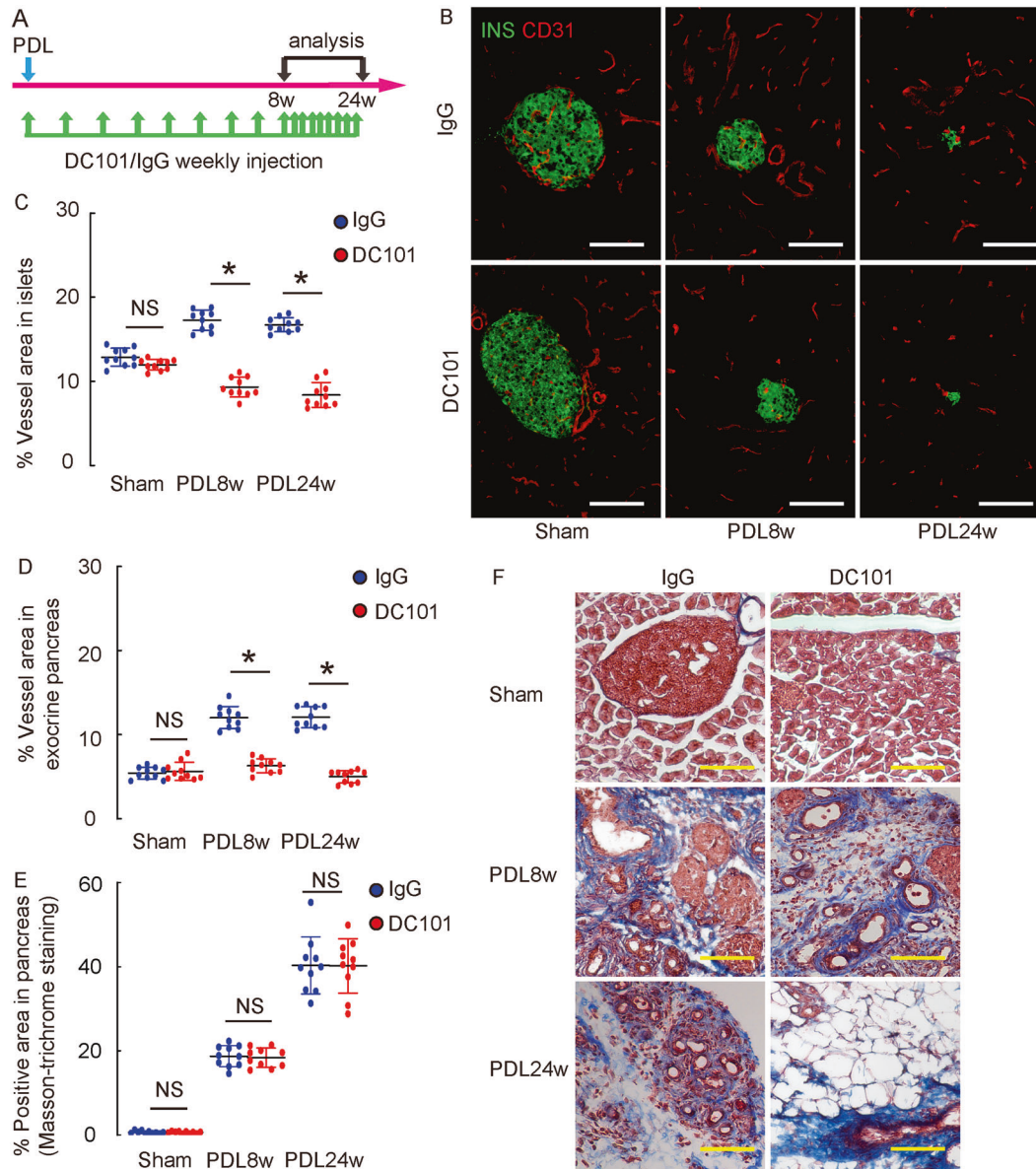


**Fig. 3** Experimental suppression of angiogenesis does not alter post-PDL fibrosis. **A** Experiment schematic: the angiogenesis was inhibited by specific antisera for VEGFR2, DC101 in PDL-treated INS1<sup>Cre</sup>; Tom; MIP-GFP mice. IgG was used as control for DC101. Mice were followed up and sacrificed at certain time points (eight weeks or 12 weeks or 24 weeks after PDL) for analysis. **B–D** Vessel density was determined based on immunostaining for CD31 and insulin, shown by representative immunofluorescent images (**B**), and by quantification in islet area (**C**) and in exocrine pancreas (**D**). **E, F** The fibrosis was assessed by Masson staining, shown by quantification (**E**), and by representative histological images (**F**). Each condition contained 10 age-matched mice, five male and five female. \* $p < 0.05$ . NS, non-significant. Scale bars are 100  $\mu$ m.

of recombination and expression of TOM, regardless they are still insulin-producing or not (e.g. not insulin-producing any more after EMT). This model allows us to distinguish normal beta-cells at the examined time (GFP+ TOM+ yellow fluorescent) from beta-cells that have undergone EMT (GFP- TOM+ red fluorescent). DC101 or control IgG was i.p. injected into the mice weekly, ever since PDL, till the end of the experiment. Mice were followed up and sacrificed at certain time points (eight weeks, 12 weeks or 24 weeks after PDL) for analysis (Fig. 3A), since we have detected start time point of beta-cell EMT at 8 weeks, peak time point of beta-cell EMT at 12 weeks and time point of nearly loss of all beta-cells at 24 weeks after PDL in our previous study<sup>9</sup>. We detected significant reduction in the increased vessel area in both the islet area (Fig. 3B, C) and the exocrine area (Fig. 3B, D), confirming the inhibitory effect of DC101 on angiogenesis. However, the fibrotic process after PDL was not seemingly affected by DC101 (Fig. 3E, F).

### Experimental suppression of angiogenesis does not alter beta-cell loss but significantly reduces the changes in beta-cell genes associated with EMT

Next, we examined whether suppression of the enhanced angiogenesis may affect the progression of beta-cell loss in the long-term PDL. We did not detect alteration in the process of reduction in beta-cell mass in PDL-tail from mice that had received DC101, compared to those that had received control IgG (Fig. 4A). However, when we examined the genes associated to EMT in isolated GFP+ beta-cells from PDL-tail pancreas at 12 weeks after PDL (the peak time point for beta-cell EMT), we found that the alteration in genes associated with EMT (E-cadherin, Snail, Slug, ZEB1 and ZEB2) were all significantly reduced in beta-cells from DC101-treated mice (Fig. 4B–F). These data suggest that suppression of angiogenesis prevents beta-cell EMT post PDL.

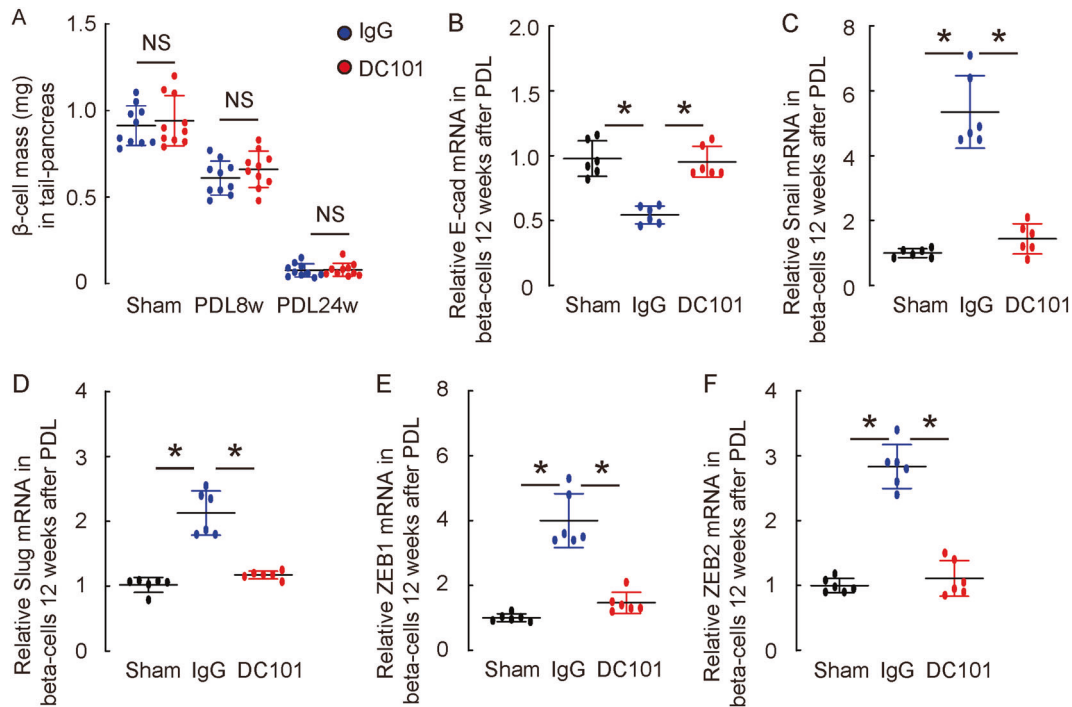


**Fig. 4** Experimental suppression of angiogenesis does not alter beta-cell loss but significantly reduces the changes in beta-cell genes associated with EMT. **A** Beta-cell mass. **B–F** RT-qPCR for E-cadherin (**B**), Snail (**C**), Slug (**D**), ZEB1 (**E**) and ZEB2 (**F**) in beta-cells from sham, PDL and IgG, and PDL and DC101-treated *INS1<sup>cre</sup>; Tom; MIP-GFP* mice at 12 weeks after surgery. Each condition contained six age-matched mice, three male and three female. \* $p < 0.05$ . NS non-significant.

#### DC101-mediated inhibition of angiogenesis abolished inflammation-induced beta-cell EMT

To evaluate whether suppression of angiogenesis indeed prevents beta-cell EMT post PDL, we examined the GFP and TOM expression in sham-treated, PDL and IgG-treated, and PDL and DC101-treated *INS1<sup>cre</sup>; Tom; MIP-GFP* mice. As mentioned before, if no beta-cell EMT occur, all beta-cells should be yellow fluorescent (TOM+ GFP+), while beta-cells that have undergone EMT will keep TOM, but lose GFP, and become red fluorescent (TOM+ GFP-). Nearly no TOM+ GFP- cells were detected in the sham-operated pancreas (Fig. 5A). However, a number of TOM+ GFP- cells were detected in the PDL and IgG-treated pancreas (Fig. 5A), suggesting presence of beta-cell EMT, consistent with our previous report<sup>15</sup>. Interestingly, again nearly no TOM+ GFP- cells were detected in PDL and DC101-treated pancreas (Fig. 5A), suggesting that DC101-mediated inhibition of angiogenesis abolishes inflammation-induced beta-cell EMT. To further confirm that the TOM+ GFP- cells in pancreas from mice received PDL and IgG are beta-cells that have undergone EMT, but not have undergone dedifferentiation towards other lineage<sup>26</sup>, the red and yellow cell populations were isolated from the digested pancreas of the PDL and DC101-treated *INS1<sup>cre</sup>; TOM; MIP-GFP* mice (Fig. 5B). Significant downregulation of E-cadherin (an epithelial cell marker) and significant upregulation of Snail, Slug, ZEB1 and ZEB2 (mesenchymal cell markers associated with cell migration) were detected in TOM+ GFP- red cells, compared to TOM+ GFP+ yellow cells, confirming that those red cells have indeed undergone EMT.

#### DC101-mediated inhibition of angiogenesis turns inflammation-induced beta-cell EMT into apoptotic beta-cell death

Finally, we examined the mechanisms underlying the beta-cell loss in PDL with suppression of angiogenesis. Since no TOM+ GFP- red cells are detected, the loss of beta-cells should result from cell death rather than phenotypic change. Apoptotic cell

death is a common mechanism of loss of beta-cells in diabetes. Thus, we assessed the apoptotic beta-cells by TUNEL staining in sham-treated, PDL and IgG-treated, and PDL and DC101-treated mice. Increases in TUNEL+ apoptotic beta-cells were not detected in PDL and IgG-treated mice, compared to the control sham-operated mice, but were detected in PDL and DC101-treated mice (Fig. 6A,B). Moreover, higher levels of cleaved caspase 9, a marker for apoptosis, were detected in islets from DC101-treated PDL-mice, compared to those from sham-treated mice or IgG-treated PDL-mice (Fig. 6C). Furthermore, increases in islet cleaved caspase 9 were not affected in DC101/PDL-treated beta-cell-specific TGF $\beta$  receptor knockout mice<sup>9</sup>, suggesting that beta-cell-apoptosis induced by angiogenesis suppression in PDL-pancreas is TGF $\beta$  receptor signaling independent (Supplementary Fig. 1). To summarize the findings in this study, the suppression of angiogenesis in PDL-pancreas prevents beta-cell EMT, leading beta-cells to apoptotic death (Fig. 6D).

#### DISCUSSION

Surgical removal of diseased pancreas together with transplantation of islets back to the patient as an autograft is the regular treatment for CP<sup>3</sup>. This therapy is, however, hindered by the difficulties in isolating islets from a fibrotic pancreas and by the poor islet function due to CPRD<sup>3</sup>. Therefore, it would be important to understand the mechanisms underlying the development of CPRD, since it could provide evidence to generate novel strategies for protecting the islet function in CP patients.

The chronic inflammation in the diseased pancreas may affect the islet integrity and function in several aspects: First, chronic inflammation may cause production and secretion of a great deal of inflammatory cytokines and peptides, which are persisting insults to the beta-cells in neighboring endocrine tissue<sup>27</sup>. It is well known that the stress on beta-cells could cause ER stress, resulting in dysfunction and even damage of beta-cells<sup>28</sup>. Second, it is also well known that the vasculature in the inflamed pancreas is

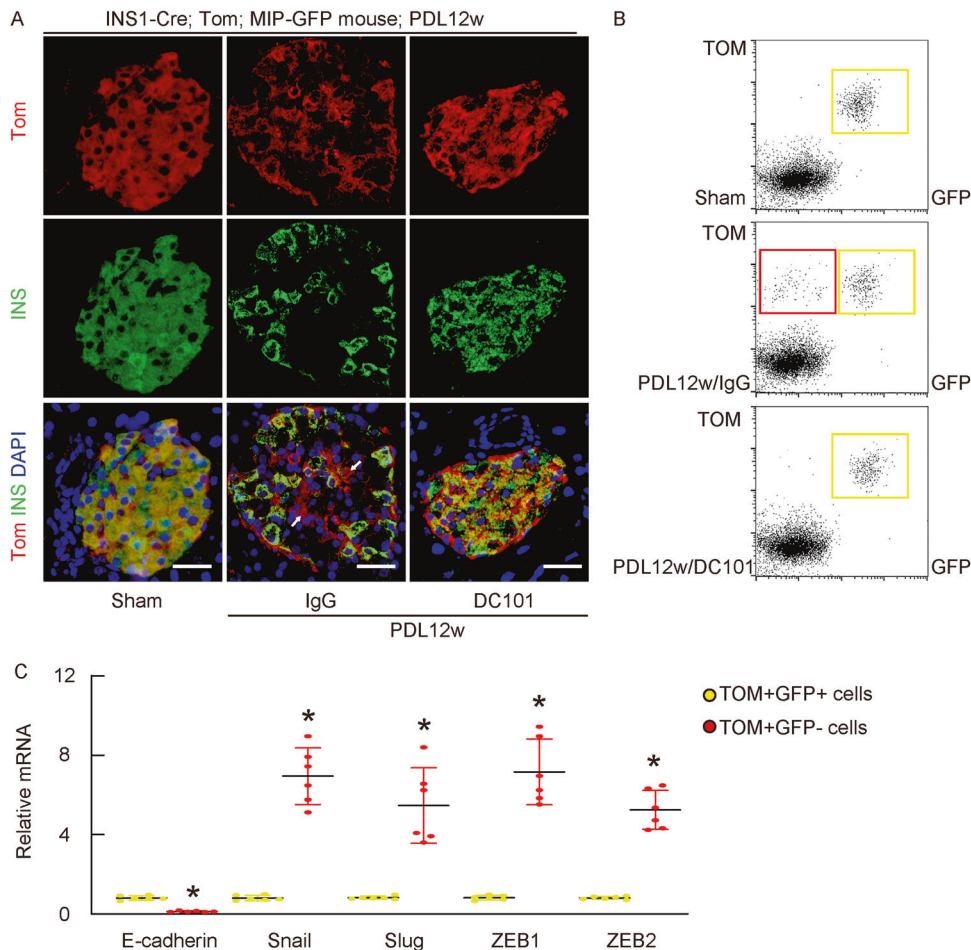


**Fig. 5 DC101-mediated inhibition of angiogenesis abolished inflammation-induced beta-cell EMT.** **A** Representative fluorescent images in sham-treated, PDL and IgG-treated, and PDL and DC101-treated  $INS1^{Cre}; TOM; MIP-GFP$  mice. **B** Representative flow charts for isolating yellow fluorescent (TOM+ GFP+) cells and red fluorescent (TOM+ GFP-) cells from sham, PDL and IgG, and PDL and DC101- treated  $INS1^{Cre}; TOM; MIP-GFP$  mice at 12 weeks after surgery. **C** The red and yellow cell populations were isolated from digested pancreas of the PDL and DC101-treated  $INS1^{Cre}; TOM; MIP-GFP$  mice and subjected to RT-qPCR analysis for E-cadherin, Snail, Slug, ZEB1 and ZEB2. Each condition contained six age-matched mice, three male and three female. \* $p < 0.05$ . Scale bars are 20  $\mu m$ .

severely affected and remodeling, since endothelia are largely regulated by cytokines and growth factors associated with inflammation, e.g. VEGF<sup>29,30</sup>. Angiogenesis is essential for progression of vessel destruction, regeneration and remodeling<sup>31</sup>. As a potent way to supply nutrients and systemic messages to the inflamed pancreas, angiogenesis plays a non-redundant role in the interaction between endocrine beta-cells and the local inflammation<sup>9,32,33</sup>.

In this study, we investigated the role of angiogenesis in beta-cell EMT induced in the inflamed PDL-pancreas<sup>4,5</sup>. The ligation site for PDL is the middle of the main pancreatic duct, which allows the non-ligated head part of the pancreas (PDL-head) minimally affected in contrast to the ligated tail part of the pancreas (PDL-tail). The intact PDL-head also allows maintenance of the supply of adequate digestive enzymes and leaves about half of the healthy islets in the normal pancreatic tissue (PDL-head) for studying the model under normoglycemia<sup>7,8</sup>. Thus, the effects by glucose metabolism on beta-cells in the inflamed pancreas have been largely avoided. Of note, in the future it may be as well interesting to look at hyperglycemic mice, for which a different model called total pancreatic duct ligation with the ligation site at the pancreatic duct close to the papilla of the duodenum is done. This total duct ligation model will cause changes in glycemia since all the islets throughout the pancreas are affected.

In an earlier study, we showed that PDL over the long-term causes a gradual loss of beta-cell mass, mimicking the phenomenon in patients with CPRD. We detected beta-cell EMT rather than beta-cell apoptosis that contributes to beta-cell loss<sup>9</sup>. Here, we further showed that when pancreatitis-associated angiogenesis was blocked, beta-cell EMT was rendered to apoptotic death. This finding may result from that some growth factors from angiogenesis support the survival of beta-cells against stress-induced damages but are not sufficient to support the maintenance of beta-cell phenotype. Therefore, beta-cells have to adapt their phenotype through an EMT in accordance with the environmental changes. On the other hand, the loss of angiogenesis-associated growth factors may reduce the survival of beta-cells under stress and may render beta-cell EMT to apoptotic beta-cell death. This notion was specifically supported by the experiments on beta-cell-specific TGF $\beta$  receptor knockout mice, since beta-cell apoptosis appeared not to be affected by inhibition of EMT in these mice. Thus, it suggests that angiogenesis in the inflamed pancreas could have a protective effect on beta-cells to prevent their apoptosis induced by stimulates, while the survived beta-cells are still under stress and may undergo EMT, which is TGF $\beta$  receptor signaling dependent. When angiogenesis is inhibited in the inflamed pancreas, beta-cells may lose those survival signals and undergo apoptosis, regardless of whether EMT is blocked or not.

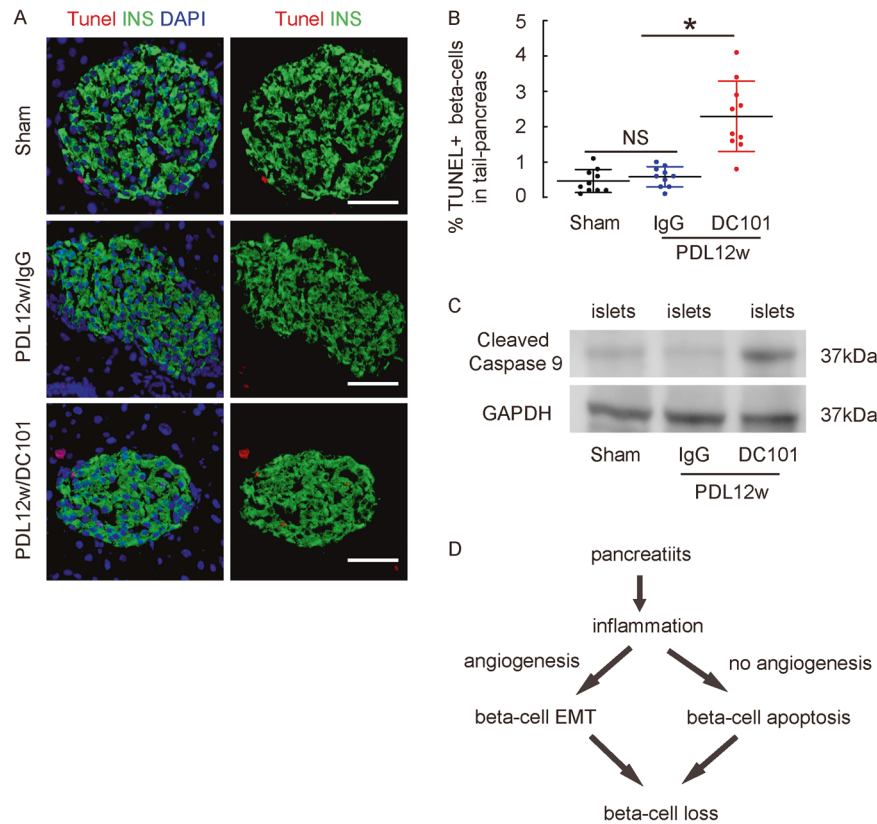


**Fig. 6 DC101-mediated inhibition of angiogenesis turns inflammation-induced beta-cell loss into apoptotic beta-cell death.** TUNEL staining was used to examine the mechanisms of beta-cell loss in PDL with suppression of angiogenesis. Sham-treated, PDL and IgG-treated, and PDL and DC101-treated mice were assessed at 12 weeks after surgery. **A**, **B** TUNEL staining was analyzed, shown by representative immunofluorescent images (**A**), and by quantification (**B**). **C** Western blot analysis of an apoptotic marker, cleaved caspase 9, in islets from sham or DC101/IgG treated PDL-mice at 12 weeks after PDL. **D** Schematic of the model: suppression of angiogenesis in the inflamed pancreas prevents beta-cell EMT, leading beta-cells to apoptotic death. Each condition contained 10 age-matched mice, five male and five female. \* $p < 0.05$ . NS, non-significant. Scale bars are 50  $\mu\text{m}$ .

Although the current study was performed in a rodent model for CP, our bioinformatic analysis also showed the importance of angiogenesis in CP patients. However, the available public database for CP or CPRD is very small. In future, if larger databases for CP or CPRD, ideally with information of clinical data on blood glucose, could be accessed for analysis, it may provide further information on the translatability of this study to human diseases.

#### DATA AVAILABILITY

All the data are presented in the article and online supplementary information. Additional information can be requested to the corresponding authors.

#### REFERENCES

- Pasca di Magliano, M. et al. Advances in acute and chronic pancreatitis: from development to inflammation and repair. *Gastroenterology* **144**, e1–e4 (2013).
- Lowenfels, A. B. et al. Pancreatitis and the risk of pancreatic cancer. International Pancreatitis Study Group. *N Engl J Med* **328**, 1433–1437 (1993).
- DiMagna, M. J. & DiMagna, E. P. Chronic pancreatitis. *Curr Opin Gastroenterol* **29**, 531–536 (2013).
- Tanaka, T. et al. New canine model of chronic pancreatitis due to chronic ischemia with incomplete pancreatic duct obstruction. *Digestion* **41**, 149–155 (1988).
- Boerma, D., Straatsburg, I. H., Offerhaus, G. J., Gouma, D. J. & van Gulik, T. M. Experimental model of obstructive, chronic pancreatitis in pigs. *Dig Surg* **20**, 520–526 (2003).
- Yamaguchi, Y., Matsuno, K., Goto, M. & Ogawa, M. In situ kinetics of acinar, duct, and inflammatory cells in duct ligation-induced pancreatitis in rats. *Gastroenterology* **104**, 1498–1506 (1993).
- Xiao, X. et al. TGFbeta receptor signaling is essential for inflammation-induced but not beta-cell workload-induced beta-cell proliferation. *Diabetes* **62**, 1217–1226 (2013).
- Xiao, X. et al. No evidence for beta cell neogenesis in murine adult pancreas. *J Clin Invest* **123**, 2207–2217 (2013).
- Xiao, X. et al. SMAD3/Stat3 signaling mediates beta-cell epithelial-mesenchymal transition in chronic pancreatitis-related. *Diabetes* **66**, 2646–2658 (2017).
- Fantozzi, A. et al. VEGF-mediated angiogenesis links EMT-induced cancer stemness to tumor initiation. *Cancer Res* **74**, 1566–1575 (2014).
- Wu, B. et al. Raddeanin A inhibited epithelial-mesenchymal transition (EMT) and angiogenesis in glioblastoma by downregulating beta-catenin expression. *International journal of medical sciences* **18**, 1609–1617 (2021).
- Carmeliet, P. & Jain, R. K. Molecular mechanisms and clinical applications of angiogenesis. *Nature* **473**, 298–307 (2011).
- Xiao, X. et al. Hypoglycemia reduces vascular endothelial growth factor a production by pancreatic Beta cells as a regulator of Beta cell mass. *J Biol Chem* **288**, 8636–8646 (2013).
- Xiao, X. et al. Pancreatic duct cells as a source of VEGF in mice. *Diabetologia* **57**, 991–1000 (2014).
- Yang, W., et al. Placental growth factor in beta cells plays an essential role in gestational beta-cell growth. *BMJ Open Diabetes Res Care* **8**, e000921 (2020).
- Wang, E. S. et al. Targeting autocrine and paracrine VEGF receptor pathways inhibits human lymphoma xenografts in vivo. *Blood* **104**, 2893–2902 (2004).
- Klement, G. et al. Continuous low-dose therapy with vinblastine and VEGF receptor-2 antibody induces sustained tumor regression without overt toxicity. *J Clin Invest* **105**, R15–R24 (2000).
- Prewett, M. et al. Antivascular endothelial growth factor receptor (fetal liver kinase 1) monoclonal antibody inhibits tumor angiogenesis and growth of several mouse and human tumors. *Cancer Res* **59**, 5209–5218 (1999).
- Thorens, B. et al. Ins1(Cre) knock-in mice for beta cell-specific gene recombination. *Diabetologia* **58**, 558–565 (2015).

20. Hara, M. et al. Transgenic mice with green fluorescent protein-labeled pancreatic beta -cells. *Am J Physiol Endocrinol Metab* **284**, E177–E183 (2003).
21. Xiao, X. et al. M2 macrophages promote beta-cell proliferation by up-regulation of SMAD7. *Proc Natl Acad Sci USA* **111**, E1211–E1220 (2014).
22. Liu, Q. et al. Insulin-positive ductal cells do not migrate into preexisting islets during pregnancy. *Exp Mol Med* <https://doi.org/10.1038/s12276-021-00593-z> (2021).
23. Barrett, T. et al. NCBI GEO: archive for functional genomics data sets—update. *Nucleic Acids Res* **41**, D991–D995 (2013).
24. Li, Z. et al. The long non-coding RNA HOTTIP promotes progression and gemcitabine resistance by regulating HOXA13 in pancreatic cancer. *J Transl Med* **13**, 84 (2015).
25. Zhou, Y. et al. Metascape provides a biologist-oriented resource for the analysis of systems-level datasets. *Nat Commun* **10**, 1523 (2019).
26. Talchai, C., Xuan, S., Lin, H. V., Sussel, L. & Accili, D. Pancreatic beta cell differentiation as a mechanism of diabetic beta cell failure. *Cell* **150**, 1223–1234 (2012).
27. DiMagno, M. J. & DiMagno, E. P. Chronic pancreatitis. *Curr Opin Gastroenterol* **28**, 523–531 (2012).
28. Coate, K. C. et al. FGF21 Is an Exocrine Pancreas Secretagogue. *Cell Metab* **25**, 472–480 (2017).
29. Berindan-Neagoe, I. et al. Molecular angiogenesis profile as a tool to discriminate chronic pancreatitis (CP) from pancreatic cancer (PC). *Pancreas* **40**, 482–483 (2011).
30. Kuehn, R., Lelkes, P. I., Bloechle, C., Niendorf, A. & Izbicki, J. R. Angiogenesis, angiogenic growth factors, and cell adhesion molecules are upregulated in chronic pancreatic diseases: angiogenesis in chronic pancreatitis and in pancreatic cancer. *Pancreas* **18**, 96–103 (1999).
31. Ferrara, N. Vascular endothelial growth factor. *Arterioscler Thromb Vasc Biol* **29**, 789–791 (2009).
32. Mateescu, G. et al. Immunohistochemical expression of growth factors in the exocrine pancreas of patients with chronic liver diseases. *Rom J Morphol Embryol* **51**, 303–307 (2010).
33. Jiang, X. et al. Pancreatic islet and stellate cells are the main sources of endocrine gland-derived vascular endothelial growth factor/prokineticin-1 in pancreatic cancer. *Pancreatol* **9**, 165–172 (2009).

## AUTHOR CONTRIBUTIONS

JQ, DT, XS, XX and CC are responsible for data acquisition and analysis; XX are responsible for study conception and design; XX drafted the manuscript and all authors agree to publication of the study. XS, XX and CC is responsible for funding and are the guarantees of the study.

## FUNDING

This work was supported by tenure-track Assistant Professor Startup from Division of Pediatric Surgery of Children's Hospital of Pittsburgh (to XX), funding of Children's Hospital of Pittsburgh of the UPMC health system (RAC; to XX), a Cochrane Weber Research Fund (to XX) and Zhejiang Provincial Natural Science Foundation of China (No: LY19H070001; to CC).

## COMPETING INTERESTS

The authors declare no competing interests.

## ETHICS APPROVAL AND CONSENT TO PARTICIPATE

All mouse experiments were approved by the Animal Research and Care Committee at the Children's Hospital of Pittsburgh and the University of Pittsburgh IACUC. No human studies were involved.

## ADDITIONAL INFORMATION

**Supplementary information** The online version contains supplementary material available at <https://doi.org/10.1038/s41374-021-00684-5>.

**Correspondence** and requests for materials should be addressed to Xiaou Shan, Xiangwei Xiao or Congde Chen.

**Reprints and permission information** is available at <http://www.nature.com/reprints>

**Publisher's note** Springer Nature remains neutral with regard to jurisdictional claims in published maps and institutional affiliations.